The Interplay Between Pore-Scale Heterogeneity, Surface Roughness, and Wettability Controls Trapping in Two-Phase Fluid Displacement in Porous Media

Geistlinger, H., Golmohammadi, S., Zulfiqar, B., Schlueter, S., Segre, E. & Holtzman, R

DOI 10.1029/2023gl106197
ISSN 0094-8276
ESSN 1944-8007

Publisher: Wiley Open Access

Geophysical Research Letters

RESEARCH LETTER
10.1029/2023GL106197

The Interplay Between Pore-Scale Heterogeneity, Surface Roughness, and Wettability Controls Trapping in Two-Phase Fluid Displacement in Porous Media

Helmut Geistlinger[1,2], Saeed Golmohammadi[2], Bilal Zulfiqar[1,2], Steffen Schlueter[1], Enrico Segre[3], and Ran Holtzman[3]

[1]Helmholtz Centre for Environmental Research-UFZ, Halle (Saale), Germany, [2]Technical University Bergakademie Freiberg, Freiberg, Germany, [3]Centre for Fluid and Complex Systems, Coventry University, Coventry, UK

Key Points:

- Interplay of pore-scale heterogeneity, wettability, and surface roughness controls displacement patterns and capillary trapping efficiency
- The invasion flow pattern for capillary flow were visualized by micro-CT- and micromodel experiments and classified in a new phase diagram
- Four generic flow regimes (phases) were observed: frontal advance, wetting and drainage invasion percolation, and ordinary percolation

Supporting Information:

Supporting Information may be found in the online version of this article.

Correspondence to:

H. Geistlinger,
helmut.geistlinger@ufz.de

Citation:

Geistlinger, H., Golmohammadi, S., Zulfiqar, B., Schlueter, S., Segre, E., & Holtzman, R. (2024). The interplay between pore-scale heterogeneity, surface roughness, and wettability controls trapping in two-phase fluid displacement in porous media. *Geophysical Research Letters*, *51*, e2023GL106197. https://doi.org/10.1029/2023GL106197

Received 14 SEP 2023
Accepted 1 DEC 2023

Author Contributions:

Conceptualization: Helmut Geistlinger
Funding acquisition: Helmut Geistlinger, Ran Holtzman
Investigation: Helmut Geistlinger, Saeed Golmohammadi, Bilal Zulfiqar
Methodology: Helmut Geistlinger, Bilal Zulfiqar
Project Administration: Helmut Geistlinger
Software: Enrico Segre, Ran Holtzman
Supervision: Helmut Geistlinger, Steffen Schlueter

Abstract Predicting the compactness of the invasion front and the amount of trapped fluid left behind is of crucial importance to applications ranging from microfluidics and fuel cells to subsurface storage of carbon and hydrogen. We examine the interplay of wettability, macro- and pore scale heterogeneity (pore angularity and pore wall roughness), and its influence on flow patterns formation and trapping efficiency in porous media by a combination of 3D micro-CT imaging with 2D direct visualization of micromodels. We observe various phase transitions between the following capillary flow regimes (phases): (a) compact advance, (b) *wetting* and *drainage* Invasion percolation, (c) Ordinary percolation.

Plain Language Summary The study of phase transitions in flow patterns that depend on the heterogeneity, wettability, and surface roughness of the pore space and their classification in phase diagrams is one of the challenges in recent multiphase flow physics. We study the dynamics of thick film and corner flows by visualization experiments with micromodels. Both flow types are characteristic of geologically representative porous media (sands, sandstones) and control the displacement and trapping process. The 2D micromodels accurately reproduce the characteristic geometric, morphological, and topological properties of 3D porous media. All microstructures were derived from μ-CT images. We fabricated identical microstructures by both DRIE-ICP etching of silicon wafers and anisotropic chemical etching of glass ceramics to vary the degree of surface roughness. The results are in excellent agreement with previous μ-CT experiments. We observe various phase transitions between the following flow regimes (phases): (a) frontal/compact advance, (b) Ordinary percolation, and (c) Invasion percolation. We show that they can be classified according to Blunt's "heterogeneity versus wettability" phase diagram.

1. Introduction

Understanding the complex patterns formed through the displacement of one fluid by another in porous materials is a fascinating scientific problem, which is also central to a wide range of natural and engineering applications across scales, from sub-mm microfluidics to km-scale water and energy resources. The displacement patterns vary widely from compact front advancing uniformly to highly ramified where invasion advances along preferential flow paths (fingers) (Juanes et al., 2020; Lenormand et al., 1988). Classifying the flow patterns in phase diagrams is one of the challenge in recent multi-phase flow research (Ben-Noah et al., 2023; Primkulov et al., 2021). Intensive research has investigated how the intricate interactions between the properties of the fluids, the solid pore surfaces, and the microstructure—the grain and pore geometry and their topology, affect the resulting patterns, displacement and trapping efficiency. In particular, experimental and numerical studies presented conflicting evidences of how wettability affects trapping efficiency in capillary flows (Chaudhary et al., 2013; Herring et al., 2016; Hu et al., 2017; Iglauer et al., 2012; Jung et al., 2016; Rahman et al., 2016; Singh et al., 2017; Trojer et al., 2015). A possible reason is the neglect of surface roughness: media with similar topological properties (e.g., Minkowski functionals) yet different surface roughness exhibit a significant difference in capillary trapping, as shown by micro-CT imaging (Geistlinger et al., 2015).

Earlier works, for example, (Blunt, 2017; Lenormand & Zarcone, 1984) that considered the effect of thick-film flow (TFF) and corner flow (CF), assumed that the pore space can be described by a straight, continuous capillary with angular rough cross section and assumed the existence of a connected, continuous film network, respectively, that is, high connectivity of small throats such that (a) unilateral films can reach the other side of the throat

Visualization: Saeed Golmohammadi, Bilal Zulfiqar, Steffen Schlueter
Writing – original draft: Helmut Geistlinger, Ran Holtzman
Writing – review & editing: Helmut Geistlinger

(geometric snap-off condition, Golmohammadi et al., 2021; Zhao et al., 2016) and that (b) precursor films can extend over larger areas of the porous medium such that trapping can occur. However, rough surfaces of sandstones (Figure 2.7 in Blunt (2017)) or glass ceramics (Geistlinger et al., 2015) exhibit a disordered micro-porous structure of interrupted grooves and crevices along the inner pore walls, that could void these assumptions.

In this letter we examine how the *microscopic* pore invasion mechanisms and heterogeneity and *macroscopic* patterns are affected by the interplay of surface roughness, as well as pore angularity, with wettability. We use micromodels of novel design that preserves the main topological and geometrical features of 3D geological media obtained from micro-CT imaging. For smooth pore wall surfaces, and uniform pore structures, for example, glass beads, we find that trapping decreases with contact angle (from imbibition to drainage). Increasing the pore-scale heterogeneity, for example, the pore angularity, we find a nonmonotonic dependence of trapping on wettability: maximal trapping in imbibition, decreasing to a minimum at neutral wettability and increasing again in drainage. This corresponds to a phase transition from *wetting* Invasion Percolation (IP) to *drainage* IP, with about the same trapping efficiency. Rough wetting pore walls doubles the trapping efficiency comparing identical pore structures. We show that this is due to a change in invasion mechanisms: spontaneous TFF followed by CF in imbibition along the rough pore surfaces provides an efficient snap-off-trapping mechanism. In drainage, the mechanism is "bypass trapping" where fingers close around and isolate clusters of wetting fluid caused by core annular flow. We also show that trapping is enhanced in 2D, due to the limited connectivity versus 3D. Trapped cluster sizes in both 2D and 3D exhibit universal scaling. We classify our experimental results using a new phase diagram proposed theoretically by Blunt (2017) (see Figure 1). As in the classical phase diagram of Lenormand et al. (1988), we show the experimental flow patterns of each phase in each quadrant of the phase diagram and derive the phase boundaries; $W \approx 1$ or $W \to \infty$, by applying the percolation laws. A detailed discussion is given in Supporting Information S1.

We use time-lapse imaging of 2D micromodels, providing the high spatio-temporal resolution required for observe TFF (typical thickness of ~10 μm). The micromodels were designed to retain the characteristic geometric, morphological, and topological properties of geologically representative media, derived from 3D micro-CT images. We note that the micro-CT images are of limited spatial (15 μm) and temporal resolution (slow acquisition), not allowing to capture the dynamics of sub-pore scale flows. Two complementary methods were used in the design: (a) direct geometrical mapping which stitch together replicated cross sections (in flow direction) of the 3D pore structures; and (b) global optimization algorithm with topological operations that produce the pore size distribution and connectivity of 3D sand (Bruecher & Bottlinger, 2006; Geistlinger & Mohammadian, 2015; Schlüter et al., 2010). The resulting micromodel dimension are $20 \times 80 \times 0.1 \times 80 \times 0.3$ mm, respectively. For details of the micromodel generation and resulting grain and pore size distribution see Supporting Information S1.

State-of-the-art manufacturing provides the desired pore geometry at high precision. Identical microstructures apart from wall smoothness were produced by two etching techniques: (a) interval-based ICP-DRIE technology was used for anisotropic etching of silicon wafer, providing extremely smooth surfaces (Figure S3 in Supporting Information S1) (Küchler et al., 2003; Zuo et al., 2013); and (b) high-precision anisotropic photolithographic etching of photosensitive glass-ceramic FOTURAN (Schott-GmbH), with rough walls (Geistlinger et al., 2019; Golmohammadi et al., 2021). Both microstructures were covered with a plain PYREX-glass plate by thermal diffusion bonding (see Supporting Information S1).

The contact angle was varied from imbibition (small) to strong drainage (very large), by using different fluid-fluid pairs: (a) water-air with $\theta = 38°$; (b) glycerin-air, 56°; (c) heptane-water, 138°; and (d) air-water, 142°. When air was used as invading fluid, Ca was calculated using the viscosity of the other, more viscous defending fluid. The contact angles are mean values of both materials, PYREX and Si; for the full physico-chemical fluid properties see Supporting Information S1. To minimize gravitational and viscous effects, the flow was horizontal and at constant flow rate (low capillary numbers, $Ca = 10^{-6}$), using syringe pump (Fusion 200, Chemyx, USA). Time lapse images were acquired in a fluorescence microscope in combination with a SLR camera (Canon EOS 5D, 100 mm Macro lens, Uranin and Oil Red dyes) and analyzed using Fiji/ImageJ (Schindelin et al., 2012).

First, we examine the effect of microscopic heterogeneity on trapping in 3D packing of glass beads and sand grains, of smooth and rough pore surfaces, respectively. For 3D bead pack, slow imbibition occurs by "frontal" advancement (FA) that is, a compact front due to cooperative filling, as observed in our micro-CT experiments (see Figure 1 and Geistlinger & Zulfiqar, 2020). Trapping of the defending, non-wetting fluid is negligible because it is well connected throughout the sample in 3D (Adler & Brenner, 1988; Wilkinson, 1984). Within

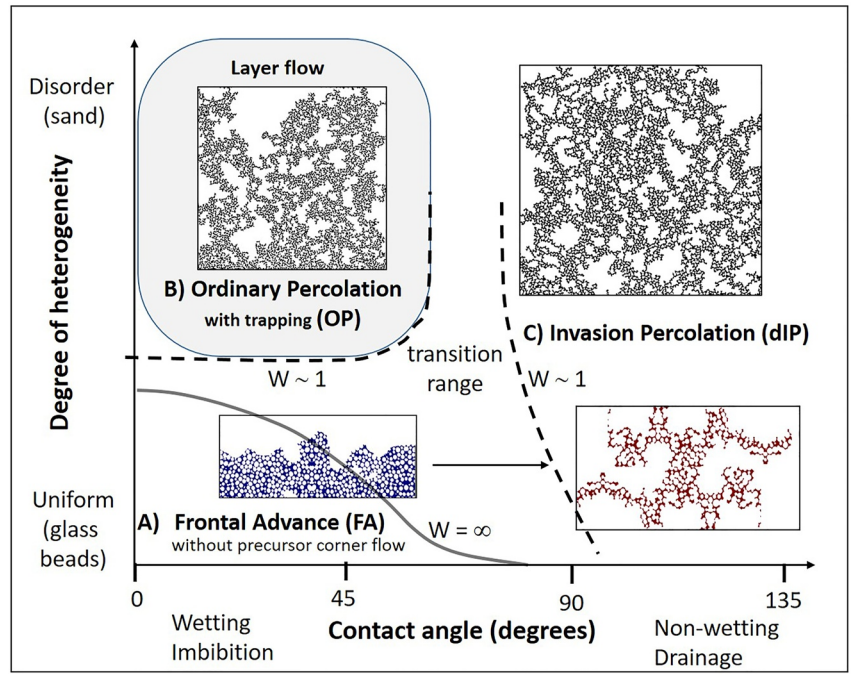

Figure 1. A phase diagram showing within the white area, where no layer flow is allowed (smooth surface), two different flow regimes: (a) frontal advance ("compact") and (c) *drainage* Invasion Percolation (dIP). For higher heterogeneity/ disorder and rougher surface (2D sand) a third flow regime is observed: Ordinary Percolation (b, gray area). The transition in displacement regimes is quantified by the finger width, W.

a narrow contact angle range (here θ = 90–100°, with critical value θ_c = 96°), trapping efficiency $S^* = S_{res}/S_{\text{norm}}$ (residual saturation S_{res} normalized by S_{norm} = 13%) changes drastically from zero to maximal trapping (Figure 2a). This transition, also denoted as the "Cieplak-Robbins (CR) transition" (Cieplak & Robbins, 1988), is characterized by a substantial, qualitative ("phase") change. For $\theta > \theta_c$ the displacement occurs by *IP*. Finger width W decreases from FA to IP, where $W \sim 1$ determines the critical contact angle (Figure 1; in agreement with (Cieplak & Robbins, 1988)). The number of large trapped clusters exhibits *universal scaling* (Wilkinson, 1984): $n(s) \sim s^{\tau}$, where s is the numbers of pores, with universal scaling exponent of τ = 2.19 in 3D (Geistlinger & Zulfiqar, 2020).

In 3D sand packings with similar topology (similar Minkowski functions, Geistlinger et al., 2015) to our glass bead packings, we observe IP displacement in drainage with similar trapping ($\theta > 100°$ in Figure 2a). In contrast,

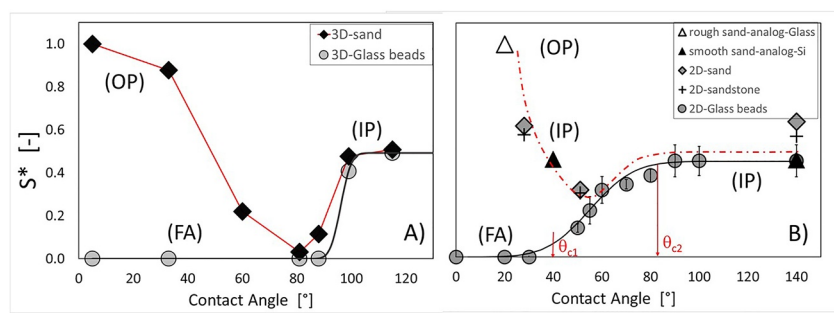

Figure 2. Non-monotonous contact angle dependency (red lines) of the normalized trapped saturation of the defending fluid S^*, in both 3D micro-CT images (a; normalized by S_{norm} = 13%) and 2D micromodel experiments (b; S_{norm} = 73%). Glass beads data in both 2D and 3D (circles) was fitted to an error function, indicating the CR transition from frontal advance to Invasion Percolation. In 3D sand and 2D sand-analogs (rough surface), the more efficient snap-off trapping is caused by spontaneous thick-film water flow during imbibition. Reduced phase connectivity in 2D enhanced trapping, for example, minimum value increases from zero in 3D to ~0.2. Increased grain angularity also increases trapping; for example, compare 2D smooth micromodel analogs of sand versus glass beads (b).

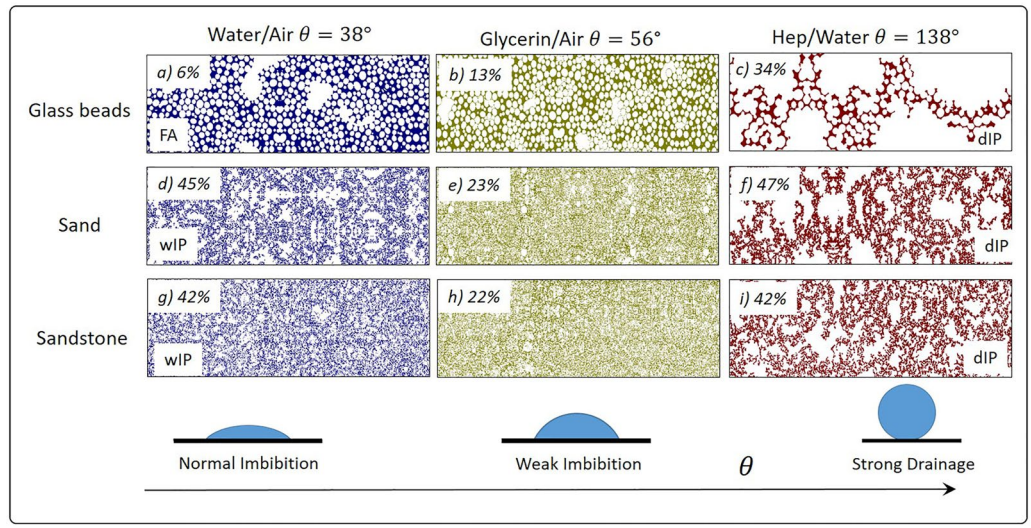

Figure 3. Macroscopic displacement patterns and trapping efficiency (residual saturation, in %) at breakthrough as function of wettability for micromodels of increasing degrees of pore space heterogeneity: rows 1–3 are 2D cross sections from glass bead packs, sand and sandstone, respectively. The invading fluid is colored, defending fluid and solid matrix not shown (white). The imbibition patterns (first column) show that with increasing pore space heterogeneity a transition from frontal advance to *wetting* (w)IP takes place. For neutral contact angles (second column) all porous media show compact displacement and less trapping (transition range in Figure 1) compared to that of *drainage* (d)IP (last column).

in strong imbibition in the 3D sand (hydrophilic grains), trapping attains a maximum which is about twice as high as in drainage, and the pattern is of ordinary percolation with trapping (Figure 1).

We hypothesize that the observed high trapping efficiency in sands is due to efficient snap-off trapping resulting from TFF and CF along the rough pore walls. A partial support for this hypothesis is provided by micro-CT images, showing that in imbibition a thick water films cover the sand grains and suggesting that the trapped air clusters are completely surrounded by a closed spherical interface, versus partial cover by convex interface in drainage (see Supporting Information S1). To test this hypothesis, we visualize the displacement in the 2D micromodels which replicate the 3D packings topology. The "2D glass beads" micromodel exhibits a similar phase transition as its 3D counterpart from compact or frontal advance (FA) to *drainage* invasion percolation (dIP) fractal pattern (Figures 3a–3c, Figure 1), with increased trapping efficiency from minimal to maximal trapping (Figure 2b). We note a few quantitative differences: in 2D, the range of contact angles where the transition occurs is larger, where the phase boundaries are $\theta_{c1} \sim 40°$ and $\theta_{c2} \sim 85°$ (Figure 2). Also, as 2D limits connectivity of defending phase, trapping is enhanced: 0.06–0.13 for $\theta = 38$–$56°$. The dependence of trapping upon the contact angle for round smooth grains (e.g., glass beads, not accounting for TFF and CF), namely the CR transition, was computed using a pore network model in (Cieplak & Robbins, 1990; Holtzman & Segre, 2015; Zhao et al., 2019) (see Figure S5 in Supporting Information S1).

In contrast to idealized media made of circular posts with smooth surfaces (i.e., 2D cross-section of the glass beads pack), the 2D micromodels representing sand and sandstone show ramified, fractal displacement fronts of *wetting* IP (Figure 3 panels d–f and g–i). This leads similar as for *drainage* IP to maximal trapping. The trapping efficiency shows a similar non-monotonic behavior as 3D sand, with maximums of ∼40% at imbibition ($\theta = 38°$) and drainage (140°), cf. Figure 2b. Another qualitative difference is that the minimal trapping efficiency is ∼20%, versus zero in 3D, due to the decreased phase connectivity in 2D. It is interesting to compare with a previous classification of patterns in smooth-surface media (excluding TFF), where the same transition from FA to wIP occurs with increasing heterogeneity/disorder (Figure 4.20 in Blunt (2017)). Increasing the contact angle from 38° to 56° leads to a dramatic change in the trapping behavior from snap-off to bypass trapping, with a drop in efficiency of ∼50% (Figure 2b). A further increase of the contact angle to 140° (strong drainage) enhances trapping again. While the macroscopic displacement regime remains similar—IP (similar to that predicted ignoring TFF, e.g., cf. Figure 4.20 in Blunt (2017)), the microscopic mechanism underlying trapping changes from by-pass by core annular flow (smooth walls) to snap-off (rough walls), see Movie S1.

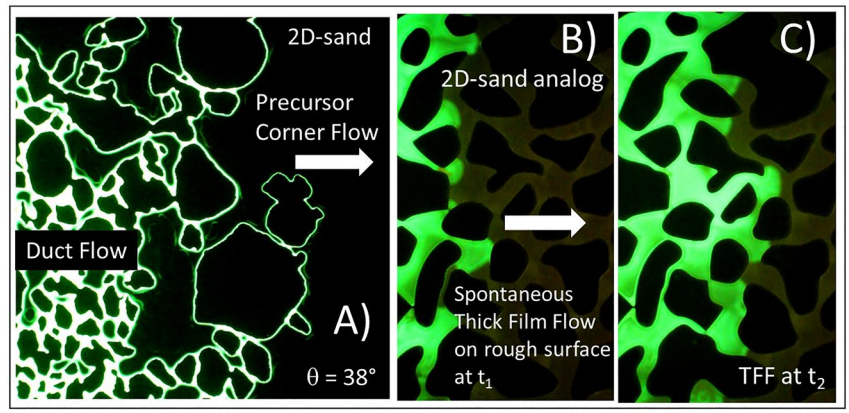

Figure 4. Microscopic wetting mechanisms captured with fluorescent microscope imaging: (a) Precursor corner flows (green rings around the front grains) in 2D sand with smooth surface in imbibition ($\theta = 38°$, see Figure 3e). Bright pores are completely filled by duct flow or by grain-grain bridging (snap-offs); (b–c) Spontaneous thick-film flow at subsequent times (marked t_1 and t_2) in 2D sand analogs made of glass ceramics (rough surfaces). In all panels, water displaces air from left to right.

The dynamics of the front advance and the bypass trapping are controlled by precursor CF with unstable grain-grain bridging (snap-off events) and subsequent duct flow (Figure 4a; also Movie S1). The more efficient snap-off trapping leads to maximum trapping efficiency during imbibition. Comparison of smooth-walled 2D micromodel analogs of glass beads and sand shows enhanced trapping due to pore *irregularity*.

Next, we address the following question: why for rough-walled 3D sand trapping is twice as high at strong imbibition that at strong drainage (Figure 2)? Based on Wenzel's argument that surface roughness enhances intrinsic wettability (Blunt, 2017; Wenzel, 1936), that is, hydrophilicity and also hydrophobicity are both enhanced, we hypothesize that the different wetting behavior on rough surfaces causes this different trapping behavior.

To test this, we compare experiments with 2D sand analogs micromodels of identical microstructure besides surface roughness. Indeed, the residual saturation in the micromodel with rough surfaces (0.73) is twofold than with smooth surfaces (0.34), see Figure 2b. The enhanced trapping is due to spontaneous precursor/prewetting flow of the invading fluid (here, water) on the rough siliceous surface, where TFF followed by CF, which is fed by TFF (vs. by duct flow in smooth surfaces), see Movie S1. However, this observation of complete wetting is surprising given the ceramic's surface intrinsic contact angle of 38°, which is expected to yield partial wetting. This can be explained by an energy argument: the change of free energy dF for a small film advance dx on a rough surface yields $dF < 0$ for contact angles smaller than $\theta_c = \arccos(1/r)$, where the roughness r is the ratio of rough to flat surface. For a typical glass ceramic roughness of 1.5 (roughness parameters $\delta = 1$ µm, $\lambda = 2$ µm, Golmohammadi et al., 2021), the critical contact angle for complete wetting is 56°; thus, for the intrinsic angle of 38°, the condition for *complete wetting* is satisfied. These observations demonstrate that invasion dynamics on rough surfaces are controlled by the temporal sequence of TFF and CF, where trapping by snap-offs occurring at random positions (due to the randomness of the throat geometry) results in a macroscopic OP behavior, whereas core annular flow leading to bypass trapping results in IP.

Our experimental data also allows us to confirm an important theoretical result: the universality of the cluster size. Since the approach to the percolation threshold is *universal*, it depends only on the spatial dimension, and not on the network structure (Blunt & Scher, 1995; Geistlinger et al., 2019; Stauffer & Aharony, 1994; Wilkinson, 1984). At the percolation threshold p_c ("terminal point") where the nonwetting fluid becomes disconnected (Blunt & Scher, 1995) and for large cluster sizes s, the cluster size distribution is expected to follow a power law decay with the Fisher exponent $\tau_{2D} = 2.05$ (Fisher, 1967; Stauffer & Aharony, 1994):

$$PDF(s, p_c) = n(s) = s^{-\tau}, \quad s \gg 1. \tag{1}$$

The complementary cumulative probability is

$$P(s) = CDF(s_{\max}) - CDF(s)) = a \cdot s^{-b}(1 - \delta), \tag{2}$$

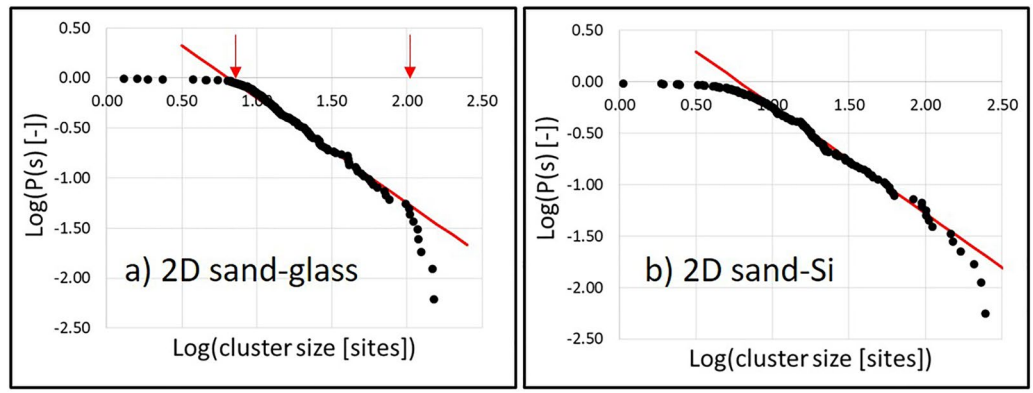

Figure 5. Universal scaling observed from the complementary cumulative probability function (CDF) versus cluster size for 2D sand analog micromodels with (a) rough and (b) smooth surface. For clusters larger than the critical size (first red arrow) the size distribution follows a power law with a critical exponent $\tau = 2.05$ (slope of the red line is $\tau - 1$). Second red arrow marks data where finite size effects become significant.

where $CDF(s)$ is the cumulative probability, $b = \tau - 1 = 1.05$, and $s_{\max}$ the maximal cluster size. For infinite cluster size, $s_{\max} \to \infty$, the residual function $\delta \simeq s/s_{\max}$ vanishes, and $\log(P(s))$ shows a linear decrease with $\log(s)$:

$$\log(P(s)) = \tilde{a} - b \cdot \log(s) - \frac{s}{s_{\max}}, \quad s < s_{\max} \tag{3}$$

where it was assumed that δ is a small quantity, such that $\log(1 - \delta) \simeq -\delta$. Our data from imbibition in the 2D sand analog micromodels for both smooth and rough pore surface is in agreement with the above theory, showing the cluster size distribution follows a power law with a critical exponent 2.05 (Figure 5; 2.19 in 3D). We note that the linear behavior that is, the universal power law only holds for cluster sizes large enough to be near the percolation threshold and small enough to exclude finite size effects. Our data shows the deviation from the linear trend for large clusters, that is, finite $s_{\max}$ (in agreement with experiments with sandstones, cf. Figure 4.30 in Blunt (2017)).

In conclusion, the presented experiments expose the microscopic mechanisms controlling trapping and hence the macroscopic displacement patterns. We show that in media with more homogeneous microstructure—round pores with smooth walls (here glass beads)—in both 2D and 3D, *compact (frontal)* advance with minimal trapping occurs in imbibition due to complete pore filling (duct flow). Increasing the contact angle causes a phase transition to *IP* regime, with increased trapping caused by invading fluid fingers bypassing pockets of the defending fluid. Increasing microscopic heterogeneity—pore angularity and wall roughness (sands and sandstone)—increases trapping, however by different mechanisms depending on roughness. For rough surfaced media, spontaneous TFF followed by CF leads to snap-off events with maximum trapping efficiency during imbibition, resulting in *OP with trapping* displacement regime. Trapping depends non-monotonically on wettability: increasing contact angle decreases trapping to a minimum at neutral wettability, which then increases again at strong drainage, where the mechanism is core annular flow leads to trapping by fingering (bypass trapping). The enhanced connectivity of 3D media was shown to dramatically decrease trapping. For both smooth and rough surfaces, our measured trapped cluster sizes exhibit universal scaling in both 2D and 3D, in agreement with theory.

We note that Singh et al. (Singh et al., 2019) discussed also the impact of heterogeneity on fluid displacement and trapping: …*"Layer flow and snap-off are both expected to become more important with increasing heterogeneity of the pore space and are thus essential to understand fluid invasion into natural porous media."*….

Finally, we note that this study considers homogenous wetting properties, and slow-enough capillary flows such that contact angle dynamics is negligible. We hypothesize that the conclusions drawn here would still hold true qualitatively for more complicated scenarios, because the competition between annular flow (through pore centers) and along crevices and corners is still expected to control trapping. It would be interesting to extend this study to consider faster flows as well as mixed- or fractional-wet media. The latter are abundant in natural geologic media due to their heterogeneous mineral composition (Geistlinger et al., 2020).

Data Availability Statement

Grain size and pore size data of 2D and 3D porous media and the physico-chemical fluid properties are available at the Figshare data repository (Geistlinger et al., 2023). Other micromodel data are available through (Golmohammadi et al., 2021) and CT-data through (Zulfiqar et al., 2020).

Acknowledgments
This work was supported by the Deutsche Forschungsgemeinschaft (GE 766/12-1 and 12-2). We thank the technicians Bernd Apelt and Max Koehne for technical help. RH acknowledges support from the Engineering and Physical Sciences Research Council (EP/V050613/1). Open Access funding enabled and organized by Projekt DEAL.

References

Adler, P. M., & Brenner, H. (1988). Multiphase flow in porous media. *Annual Review of Fluid Mechanics*, *20*(1), 35–59. https://doi.org/10.1146/annurev.fl.20.010188.000343

Ben-Noah, I., Friedman, S. P., & Berkowitz, B. (2023). Dynamics of air flow in partially water-saturated porous media. *Reviews of Geophysics*, *61*(2), e2022RG000798. https://doi.org/10.1029/2022rg000798

Blunt, M. J. (2017). *Multiphase flow in permeable media: A pore-scale perspective*. Cambridge University Press.

Blunt, M. J., & Scher, H. (1995). Pore-level modeling of wetting. *Physical review E*, *52*(6), 6387–6403. https://doi.org/10.1103/PhysRevE.52.6387

Bruecher, M., & Bottlinger, M. (2006). Dreidimensionale computersimulation zur untersuchung von partikelschüttungen aus unregelmäßig geformten partikeln. *Chemie Ingenieur Technik*, *78*(6), 727–733. https://doi.org/10.1002/cite.200500185

Chaudhary, K., Bayani Cardenas, M., Wolfe, W. W., Maisano, J. A., Ketcham, R. A., & Bennett, P. C. (2013). Pore-scale trapping of supercritical CO_2 and the role of grain wettability and shape. *Geophysical Research Letters*, *40*(15), 3878–3882. https://doi.org/10.1002/grl.50658

Cieplak, M., & Robbins, M. O. (1988). Dynamical transition in quasistatic fluid invasion in porous media. *Physical Review Letters*, *60*(20), 2042–2045. https://doi.org/10.1103/PhysRevLett.60.2042

Cieplak, M., & Robbins, M. O. (1990). Influence of contact angle on quasistatic fluid invasion of porous media. *Physical Review B*, *41*(16), 11508–11521. https://doi.org/10.1103/PhysRevB.41.11508

Fisher, M. E. (1967). The theory of condensation and the critical point. *Physics Physique Fizika*, *3*(5), 255–283. https://doi.org/10.1103/PhysicsPhysiqueFizika.3.255

Geistlinger, H., Ataei-Dadavi, I., Mohammadian, S., & Vogel, H.-J. (2015). The impact of pore structure and surface roughness on capillary trapping for 2-D and 3-D porous media: Comparison with percolation theory. *Water Resources Research*, *51*(11), 9094–9111. https://doi.org/10.1002/2015wr017852

Geistlinger, H., Ding, Y., Apelt, B., Schlüter, S., Küchler, M., Reuter, D., et al. (2019). Evaporation study based on micromodel experiments: Comparison of theory and experiment. *Water Resources Research*, *55*(8), 6653–6672. https://doi.org/10.1029/2018WR024647

Geistlinger, H., Golmohammadi, S., Zulfiqar, B., Schlueter, S., Segre, E., & Holtzman, R. (2023). The interplay between pore-scale heterogeneity, surface roughness and wettability controls trapping in two-phase fluid displacement in porous media [Dataset]. Geophysical Research Letters, Figshare. https://doi.org/10.6084/m9.figshare.24486598.v1

Geistlinger, H., & Mohammadian, S. (2015). Capillary trapping mechanism in strongly water wet systems: Comparison between experiment and percolation theory. *Advances in Water Resources*, *79*, 35–50. https://doi.org/10.1016/j.advwatres.2015.02.010

Geistlinger, H., & Zulfiqar, B. (2020). The impact of wettability and surface roughness on fluid displacement and capillary trapping in 2-D and 3-D porous media: 1. Wettability-controlled phase transition of trapping efficiency in glass beads packs. *Water Resources Research*, *56*(10), e2019WR026826. https://doi.org/10.1029/2019WR026826

Geistlinger, H., Zulfiqar, B., & Amro, M. (2020). New structural percolation transition in fractional wet 3D porous media: A μ-ct study. *Water Resources Research*, *56*(10), e2019WR026826. https://doi.org/10.1029/2021WR030037

Golmohammadi, S., Ding, Y., Kuechler, M., Reuter, D., Schlueter, S., Amro, M., & Geistlinger, H. (2021). Impact of wettability and gravity on fluid displacement and trapping in representative 2D micromodels of porous media (2D sand analogs). *Water Resources Research*, *57*(10), 6653–6672. https://doi.org/10.1029/2021WR029908

Herring, A. L., Sheppard, A., Andersson, L., & Wildenschild, D. (2016). Impact of wettability alteration on 3D nonwetting phase trapping and transport. *International Journal of Greenhouse Gas Control*, *46*, 175–186. https://doi.org/10.1016/j.ijggc.2015.12.026

Holtzman, R., & Segre, E. (2015). Wettability stabilizes fluid invasion into porous media via nonlocal, cooperative pore filling. *Physical Review Letters*, *115*(16), 164501. https://doi.org/10.1103/PhysRevLett.115.164501

Hu, R., Wan, J., Kim, Y., & Tokunaga, T. K. (2017). Wettability impact on supercritical CO_2 capillary trapping: Pore-scale visualization and quantification. *Water Resources Research*, *53*(8), 6377–6394. https://doi.org/10.1002/2017WR020721

Iglauer, S., Fernø, M., Shearing, P., & Blunt, M. (2012). Comparison of residual oil cluster size distribution, morphology and saturation in oil-wet and water-wet sandstone. *Journal of Colloid and Interface Science*, *375*(1), 187–192. https://doi.org/10.1016/j.jcis.2012.02.025

Juanes, R., Meng, Y., & Primkulov, B. K. (2020). Multiphase flow and granular mechanics. *Physical Review Fluids*, *5*(11), 110516. https://doi.org/10.1103/PhysRevFluids.5.110516

Jung, M., Brinkmann, M., Seemann, R., Hiller, T., de La Lama, M. S., & Herminghaus, S. (2016). Wettability controls slow immiscible displacement through local interfacial instabilities. *Physical Review Fluids*, *1*(7), 074202. https://doi.org/10.1103/PhysRevFluids.1.074202

Küchler, M., Otto, T., Gessner, T., Ebling, F., & Schröder, H. (2003). Hot embossing for MEMS using silicon tools. *International Journal of Computational Engineering Science*, *4*(03), 609–612. https://doi.org/10.1142/S1465876303001873

Lenormand, R., Touboul, E., & Zarcone, C. (1988). Numerical models and experiments on immiscible displacements in porous media. *Journal of Fluid Mechanics*, *189*, 165–187. https://doi.org/10.1017/S0022112088000953

Lenormand, R., & Zarcone, C. (1984). Role of roughness and edges during imbibition in square capillaries. In *SPE annual technical conference and exhibition*. https://doi.org/10.2118/13264-MS

Primkulov, B. K., Pahlavan, A. A., Fu, X., Zhao, B., MacMinn, C. W., & Juanes, R. (2021). Wettability and Lenormand's diagram. *Journal of Fluid Mechanics*, *923*, A34. https://doi.org/10.1017/jfm.2021.579

Rahman, T., Lebedev, M., Barifcani, A., & Iglauer, S. (2016). Residual trapping of supercritical CO_2 in oil-wet sandstone. *Journal of Colloid and Interface Science*, *469*, 63–68. https://doi.org/10.1016/j.jcis.2016.02.020

Schindelin, J., Arganda-Carreras, I., Frise, E., Kaynig, V., Longair, M., Pietzsch, T., et al. (2012). Fiji: An open-source platform for biological-image analysis. *Nature Methods*, *9*(7), 676–682. https://doi.org/10.1038/nmeth.2019

Schlüter, S., Weller, U., & Vogel, H.-J. (2010). Segmentation of X-ray microtomography images of soil using gradient masks. *Computers & Geosciences*, *36*(10), 1246–1251. https://doi.org/10.1016/j.cageo.2010.02.007

Singh, K., Jung, M., Brinkmann, M., & Seemann, R. (2019). Capillary-dominated fluid displacement in porous media. *Annual Review of Fluid Mechanics*, *51*(1), 429–449. https://doi.org/10.1146/annurev-fluid-010518-040342

Singh, K., Scholl, H., Brinkmann, M., Michiel, M. D., Scheel, M., Herminghaus, S., & Seemann, R. (2017). The role of local instabilities in fluid invasion into permeable media. *Scientific Reports*, *7*(1), 1–11. https://doi.org/10.1038/s41598-017-00191-y

Stauffer, D., & Aharony, A. (1994). *Introduction to percolation theory*. Taylor & Francis. https://doi.org/10.1201/9781315274386

Trojer, M., Szulczewski, M. L., & Juanes, R. (2015). Stabilizing fluid-fluid displacements in porous media through wettability alteration. *Physical Review Applied*, *3*(5), 054008. https://doi.org/10.1103/PhysRevApplied.3.054008

Wenzel, R. N. (1936). Resistance of solid surfaces to wetting by water. *Industrial & Engineering Chemistry*, *28*(8), 988–994. https://doi.org/10.1021/ie50320a024

Wilkinson, D. (1984). Percolation model of immiscible displacement in the presence of buoyancy forces. *Physical Review A*, *30*(1), 520–531. https://doi.org/10.1103/PhysRevA.30.520

Zhao, B., MacMinn, C. W., & Juanes, R. (2016). Wettability control on multiphase flow in patterned microfluidics. *Proceedings of the National Academy of Sciences*, *113*(37), 10251–10256. https://doi.org/10.1073/pnas.1603387113

Zhao, B., MacMinn, C. W., Primkulov, B. K., Chen, Y., Valocchi, A. J., Zhao, J., et al. (2019). Comprehensive comparison of pore-scale models for multiphase flow in porous media. *Proceedings of the National Academy of Sciences*, *116*(28), 13799–13806. https://doi.org/10.1073/pnas.1901619116

Zulfiqar, B., Vogel, H., Ding, Y., Golmohammadi, S., Küchler, M., Reuter, D., & Geistlinger, H. (2020). The impact of wettability and surface roughness on fluid displacement and capillary trapping in 2-D and 3-D porous media: 2. Combined effect of wettability, surface roughness, and pore space structure on trapping efficiency in sand packs and micromodels. *Water Resources Research*, *56*(10), e2020WR027965. https://doi.org/10.1029/2020WR027965

Zuo, L., Zhang, C., Falta, R. W., & Benson, S. M. (2013). Micromodel investigations of CO_2 exsolution from carbonated water in sedimentary rocks. *Advances in Water Resources*, *53*, 188–197. https://doi.org/10.1016/j.advwatres.2012.11.004